The Canadian Mineralogist
Vol. 35, pp. 777-784 (1997)

THE CRYSTAL STRUCTURE OF WICKSITE

MARK A. COOPER[1] AND FRANK C. HAWTHORNE

Department of Geological Sciences, University of Manitoba, Winnipeg, Manitoba R3T 2N2

ABSTRACT

The crystal structure of wicksite, orthorhombic, *a* 12.524(1), *b* 12.907(2), *c* 11.646(2) Å, *V* 1882.4(4) Å^3, *Pcab*, has been solved by direct methods and refined to an *R* index of 2.4% based on 2413 observed reflections measured with Mo*K*α X-radiation. The crystal used in the collection of the X-ray intensity data was analyzed with an electron microprobe, giving the formula $4[NaCa_2(Fe^{2+}_{1.58}Mg_{0.42})(Fe^{2+}_{0.46}\ Fe^{3+}_{0.82}Al_{0.18}Mg_{0.54})(Fe^{2+}_{1.40}Mn^{2+}_{0.60})(PO_4)_6(H_2O)_2]$. Wicksite is the iron phosphate analogue of grischunite, ideally $4[NaCa_2Mn^{2+}(Mn^{2+}_{0.5}Fe^{3+}_{0.5})_2(AsO_4)_6(H_2O)_2]$. The unique sites include three tetrahedrally coordinated *P* sites, four octahedrally coordinated sites, one nine-coordinated *Ca* site and one H_2O group. The octahedrally coordinated sites have the following occupancies: *M*(1) is occupied by Fe^{2+} and Mg, *M*(2) is occupied by (Fe^{2+},Mg) and (Fe^{3+},Al) in equal amounts, *M*(3) is occupied by Fe^{2+} and Mn^{2+}, and *Na* is occupied by Na. The *Ca* site is coordinated by eight O atoms and an H_2O group. Wicksite is a densely packed heteropolyhedral structure with extensive edge-sharing between *M* and *Ca* polyhedra, and corner-sharing between *P* tetrahedra and *M* octahedra. Attempts to refine the structures of both wicksite and grischunite in monoclinic symmetry were inconclusive, despite the fact that wicksite has optical properties that suggest monoclinic symmetry.

Keywords: wicksite, crystal structure, electron-microprobe analysis, site populations, phosphate, grischunite, arsenate.

SOMMAIRE

Nous avons affiné la structure cristalline de la wicksite, orthorhombique, *a* 12.524(1), *b* 12.907(2), *c* 11.646(2) Å, *V* 1882.4(4) Å^3, *Pcab*, par méthodes directes jusqu'à un résidu *R* de 2.4% en utilisant 2413 réflexions observées, mesurées avec un rayonnement Mo*K*α. Le cristal qui a servi pour la collection des intensités de diffraction X a été analysé avec une microsonde électronique; sa formule serait: $4[NaCa_2(Fe^{2+}_{1.58}Mg_{0.42})(Fe^{2+}_{0.46}Fe^{3+}_{0.82}Al_{0.18}Mg_{0.54})(Fe^{2+}_{1.40}Mn^{2+}_{0.60})(PO_4)_6(H_2O)_2]$. La wicksite est le phosphate de fer analogue à la grischunite, qui possède la formule idéale $4[NaCa_2Mn^{2+}(Mn^{2+}_{0.5}Fe^{3+}_{0.5})_2(AsO_4)_6(H_2O)_2]$. Parmi les sites uniques, il y a trois sites *P* à coordinence tétraédrique, quatre sites à coordinence octaédrique, un site *Ca* à coordinence 9, et un groupe H_2O. Les sites à coordinence octaédrique sont les suivants: *M*(1), occupé par Fe^{2+} et Mg, *M*(2), occupé par (Fe^{2+},Mg) et (Fe^{3+},Al) en proportions égales, *M*(3), occupé par Fe^{2+} et Mn^{2+}, et *Na*, occupé par Na. Le site *Ca* est coordonné par huit atomes d'oxygène et un groupe H_2O. La wicksite a une structure à empilement dense de hétéropolyèdres; les polyèdres *M* et *Ca* partagent plusieurs de leurs arêtes, et les tétraèdres *P* et les octaèdres *M* partagent des coins. Nous avons essayé d'affiner la structure de la wicksite et de la grischunite dans le système monoclinique; les résultats n'ont pas été concluants, malgré le fait que certaines des propriétés optiques de la wicksite semblent indiquer une symétrie monoclinique.

(Traduit par la Rédaction)

Mots-clés: wicksite, structure cristalline, données de microsonde électronique, population des sites, phosphate, grischunite, arsenate.

INTRODUCTION

Wicksite is a hydrated Fe-phosphate mineral described by Sturman *et al.* (1981) from the Big Fish River in northeastern Yukon Territory. It occurs as blue plates in nodules in bedded ironstone and shale, and is intimately associated with wolfeite, satterlyite and maricite. The general geology of the region was described by Young (1977), and a detailed description was given by Robertson (1982) and Robinson *et al.* (1992). The crystal structure of wicksite has been solved as part of our general program on the structures of oxysalt minerals, and the results are reported here.

EXPERIMENTAL

Careful optical examination in non-polarized, polarized and cross-polarized light identified a single crystal of good quality, and this was then ground to a sphere of diameter 0.20 mm using a Bond sphere-grinder. The

[1] *E-mail address*: macooper@bldgwall.lan1.umanitoba.ca

crystal was mounted on a Siemens *P*4 automated four-circle diffractometer and aligned using thirty-one relatively intense reflections. The orientation matrix and cell dimensions were determined from the setting angles by least-squares refinement; the cell dimensions given in Table 1 are for the space group *Pcab* and are in a different orientation from those given by Sturman *et al.* (1981). Data were collected, and the structure was solved in the latter orientation, but the data were subsequently transformed from *Pbca* to *Pcab* in order to correspond to the setting for grischunite, with which wicksite is isostructural. A total of 7333 reflections were collected over the index ranges $\bar{2} \le h \le 17$, $\bar{2} \le k \le 18$, $\bar{16} \le l \le 16$ with scan speeds between 3.0 and 30.0°2θ/min. and over the range $4 \le 2\theta \le 60°$. Subsequent to the collection of θ–2θ data, psi-scan data were collected for 18 reflections at 4° intervals of psi. The psi-scan data were corrected for absorption, modeling the crystal as an ellipsoid and reducing *R*(azimuthal) from 0.83 to 0.70%. The θ–2θ intensity data were corrected for absorption, Lorentz, polarization and background effects, averaged and reduced to structure factors; of the 2763 unique reflections, 2413 were considered as observed ($|F_o| > 5\sigma|F_o|$).

Following collection of the X-ray intensity data, the crystal was mounted in epoxy, ground, polished, carbon-coated and analyzed with an electron microprobe according to the method of Hawthorne *et al.* (1993).

TABLE 1. MISCELLANEOUS INFORMATION FOR WICKSITE

a (Å)	12.524(1)	Crystal size (mm)	0.20 mm sphere
b	12.907(2)	Radiation	Mo*K*α/Graphite
c	11.646(2)	Total no. of I	7333
V (Å^3)	1882.4(4)	No. of $\|F\|$	2763
Space Group	*Pcab*	No. of $\|F_o\| > 5\sigma$	2413
μ (mm^{-1})	4.89	*R*(azimuthal) %	0.83 - 0.70
		R(merge) %	3.3
		R(obs) %	2.4
		wR(obs) %	2.1

Cell content: $4[NaCa_2(Fe^{2+}_{1.68}Mg_{0.42})(Fe^{3+}_{0.48}Fe^{3+}_{0.82}Al_{0.18}Mg_{0.54})(Fe^{2+}_{1.40}Mn^{2+}_{0.60})(PO_4)_8(H_2O)_2]$

$R = \Sigma(||F_o|-|F_c||)/\Sigma|F_o|$

$wR = [\Sigma w(|F_o|-|F_c|)^2/\Sigma F_o^2]^{1/2}$, $w = 1/\sigma^2 F_o \cdot [1-\exp(-2.7(\sin\theta/\lambda)^2)]$

Structure Solution and Refinement

All calculations were done with the SHELXTL PC Plus system of programs; *R* and *wR* indices are of the conventional form and are given as percentages. The structure was solved by direct methods. The *E* statistics indicate that the structure is centrosymmetric, and systematic absences are compatible with the space group *Pcab*. The solution with the highest combined figure-of-merit proved to be correct, and the structure was refined by a combination of least-squares refinement and difference-Fourier synthesis to an *R* index of 2.4%. At

TABLE 2. FINAL POSITONAL AND DISPLACEMENT (Å x 10^4) PARAMETERS FOR WICKSITE

Site	*x*	*y*	*z*	U_{eq}	U_{11}	U_{22}	U_{33}	U_{23}	U_{13}	U_{12}
P(1)	0.39144(4)	0.30143(4)	0.22496(4)	74(1)	74(2)	79(2)	68(2)	−6(2)	−1(2)	−1(2)
P(2)	0.10100(4)	0.44304(4)	0.25356(4)	74(1)	79(2)	72(2)	71(2)	−1(2)	−2(2)	1(2)
P(3)	0.26745(4)	0.12409(4)	0.47592(4)	84(1)	102(2)	69(2)	81(2)	−1(2)	−10(2)	−1(2)
M(1)	0.15443(3)	0.20669(2)	0.22665(3)	91(1)	85(2)	83(2)	105(2)	11(1)	9(1)	6(1)
M(2)	0.33291(3)	0.04305(3)	0.22587(3)	71(1)	73(2)	72(2)	70(2)	−3(1)	−1(1)	6(1)
M(3)	0.02571(3)	0.26873(3)	0.45508(2)	148(1)	207(2)	138(2)	100(1)	2(1)	−24(1)	−71(1)
Ca	0.26395(3)	0.37404(3)	0.49346(3)	113(1)	120(2)	117(2)	103(2)	16(1)	−12(1)	−14(2)
Na	0	0	0	332(5)	232(8)	372(9)	392(8)	226(7)	−47(7)	72(7)
O(1)	0.4989(1)	0.2754(1)	0.2820(1)	114(3)	86(6)	144(6)	114(5)	−3(5)	−20(5)	17(5)
O(2)	0.4092(1)	0.3380(1)	0.1008(1)	119(4)	145(7)	138(7)	73(6)	11(5)	16(5)	15(6)
O(3)	0.3216(1)	0.2027(1)	0.2215(1)	131(4)	105(6)	122(7)	164(6)	−1(6)	−2(6)	−24(6)
O(4)	0.3358(1)	0.3850(1)	0.2973(1)	117(4)	103(7)	139(7)	110(5)	−37(5)	7(5)	15(6)
O(5)	0.1660(1)	0.5444(1)	0.2551(1)	124(4)	163(7)	78(6)	132(6)	6(5)	8(6)	−27(6)
O(6)	0.1550(1)	0.3625(1)	0.1765(1)	100(3)	113(7)	99(6)	88(5)	−15(5)	6(5)	6(6)
O(7)	0.0938(1)	0.4034(1)	0.3784(1)	110(4)	144(7)	116(6)	72(5)	11(5)	6(5)	5(6)
O(8)	−0.0097(1)	0.4660(1)	0.2013(1)	157(4)	122(7)	193(7)	155(7)	3(5)	−25(6)	49(6)
O(9)	0.1923(1)	0.2033(1)	0.4165(1)	118(4)	139(7)	100(6)	114(5)	16(5)	−5(5)	23(6)
O(10)	0.3527(1)	0.1897(1)	0.5400(1)	144(4)	162(7)	144(7)	125(6)	−22(5)	−19(6)	−54(6)
O(11)	0.2009(1)	0.0519(1)	0.5539(1)	127(4)	165(7)	88(6)	126(6)	16(5)	−12(6)	−31(6)
O(12)	0.3297(1)	0.0509(1)	0.3959(1)	154(4)	184(8)	152(7)	127(6)	−37(5)	−34(6)	78(7)
O(13)	−0.0276(1)	0.1165(1)	0.4864(1)	151(4)	186(8)	143(6)	124(6)	17(5)	2(6)	20(7)
H(1)	0.013(4)	0.085(4)	0.549(3)	700(100)*						
H(2)	−0.007(4)	0.074(3)	0.421(3)	700(100)*						

* constrained to be equal.

this stage, we noted that the $M(2)$ site was occupied by ~0.5 (Fe^{2+} + Mg) and ~0.5 (Fe^{3+} + Al). We also discovered that wicksite is isostructural with grischunite, and that the corresponding site in grischunite is occupied by 0.50 Mn^{2+} + 0.50 Fe^{3+} (Bianchi *et al.* 1987). This led us to suspect that both minerals are monoclinic, with ordering of M^{2+} and M^{3+} at separate sites. We collected intensity data for grischunite as well, but were unable to justify the use of monoclinic symmetry in the refinement of either wicksite or grischunite. Consequently, we report the orthorhombic model for wicksite. Final atomic parameters are listed in Table 2, and selected interatomic distances and angles are given in Table 3. A bond-valence table, calculated from the parameters of Brown & Altermatt (1985), is shown as Table 4. Observed and calculated structure-factors may be obtained from The Depository of Unpublished Data, CISTI, National Research Council, Ottawa, Ontario K1A 0S2.

Chemical Composition

The results of electron-microprobe analysis are given in Table 5. The unit formula was calculated on the basis of 26 anions *pfu* (per formula unit). The H_2O content was calculated as 2 groups *pfu*, as indicated by the crystal-structure solution. The Fe^{3+} content was initially calculated to produce cations and cation sums as close to integer values as possible (*i.e.*, P ≈ 6, Na ≈ 1, Ca ≈ 2, Mg + Fe^{2+} + Fe^{3+} + Al + Mn^{2+} ≈ 6). This produced

TABLE 3. SELECTED INTERATOMIC DISTANCES (Å) AND ANGLES (°) IN WICKSITE

P(1)–O(1)	1.538(2)	*M*(1)–O(1)a	2.065(2)		
P(1)–O(2)	1.537(1)	*M*(1)–O(3)	2.095(2)		
P(1)–O(3)	1.547(2)	*M*(1)–O(5)b	2.110(2)		
P(1)–O(4)	1.536(2)	*M*(1)–O(6)	2.094(1)		
<*P*(1)–O>	1.540	*M*(1)–O(9)	2.262(1)		
		M(1)–O(10)c	2.186(1)		
P(2)–O(5)	1.541(2)	<*M*(1)–O>	2.135		
P(2)–O(6)	1.531(2)				
P(2)–O(7)	1.543(1)	*M*(2)–O(3)	2.065(2)		
P(2)–O(8)	1.543(2)	*M*(2)–O(4)b	2.058(2)		
<*P*(2)–O>	1.540	*M*(2)–O(5)b	2.103(2)		
		M(2)–O(8)d	1.995(2)		
P(3)–O(9)	1.552(2)	*M*(2)–O(11)c	2.050(1)		
P(3)–O(10)	1.553(2)	*M*(2)–O(12)	1.983(1)		
P(3)–O(11)	1.546(2)	<*M*(2)–O>	2.042		
P(3)–O(12)	1.540(2)				
<*P*(3)–O>	1.548	*M*(3)–O(1)a	2.121(1)		
		M(3)–O(2)e	2.084(1)		
Ca–O(2)e	2.546(2)	*M*(3)–O(7)	2.133(2)		
Ca–O(4)	2.460(1)	*M*(3)–O(9)	2.296(2)		
Ca–O(6)e	2.368(1)	*M*(3)–O(10)a	2.442(2)		
Ca–O(7)	2.546(2)	*M*(3)–O(13)	2.107(2)		
Ca–O(9)	2.543(2)	<*M*(3)–O>	2.197		
Ca–O(10)	2.681(2)				
Ca–O(11)h	2.401(2)	*Na*–O(2)a,f	2.654(2)	x2	
Ca–O(12)h	2.872(2)	*Na*–O(7)b,g	2.223(2)	x2	
Ca–O(13d)	2.615(2)	*Na*–O(12)c,i	2.540(2)	x2	
<*Ca*–O>	2.559	<*Na*–O>	2.472		
P(1) tetrahedron					
O(1)–O(2)	2.524(2)	O(1)–*P*(1)–O(2)	110.3(1)		
O(1)–O(3)	2.512(2)	O(1)–*P*(1)–O(3)	109.0(1)		
O(1)–O(4)	2.491(2)	O(1)–*P*(1)–O(4)	108.2(1)		
O(2)–O(3)	2.497(2)	O(2)–*P*(1)–O(3)	108.1(1)		
O(2)–O(4)	2.540(2)	O(2)–*P*(1)–O(4)	111.5(1)		
O(3)–O(4)	2.520(2)	O(3)–*P*(1)–O(4)	109.7(1)		
<O–O>	2.514	<O–*P*(1)–O>	109.5		
P(2) tetrahedron					
O(5)–O(6)	2.524(2)	O(5)–*P*(2)–O(6)	110.5(1)		
O(5)–O(7)	2.487(2)	O(5)–*P*(2)–O(7)	107.5(1)		
O(5)–O(8)	2.501(2)	O(5)–*P*(2)–O(8)	108.4(1)		
O(6)–O(7)	2.528(2)	O(6)–*P*(2)–O(7)	110.7(1)		
O(6)–O(8)	2.474(2)	O(6)–*P*(2)–O(8)	107.2(1)		
O(7)–O(8)	2.566(2)	O(7)–*P*(2)–O(8)	112.5(1)		
<O–O>	2.513	<O–*P*(2)–O>	109.5		

Table 3. cont.

P(3) tetrahedron					
O(9)–O(10)	2.476(2)	O(9)–*P*(3)–O(10)	105.8(1)		
O(9)–O(11)	2.528(2)	O(9)–*P*(3)–O(11)	109.4(1)		
O(9)–O(12)	2.624(2)	O(9)–*P*(3)–O(12)	116.2(1)		
O(10)–O(11)	2.609(2)	O(10)–*P*(3)–O(11)	114.6(1)		
O(10)–O(12)	2.472(2)	O(10)–*P*(3)–O(12)	106.1(1)		
O(11)–O(12)	2.448(2)	O(11)–*P*(3)–O(12)	105.0(1)		
<O–O>	2.526	<O–*P*(3)–O>	109.5		
M(1) octahedron					
O(1)a–O(5)b	3.158(2)	O(1)a–*M*(1)–O(5)b	98.3(1)		
O(1)a–O(6)	2.915(2)	O(1)a–*M*(1)–O(6)	89.0(1)		
O(1)a–O(9)	2.898(2)	O(1)a–*M*(1)–O(9)	84.0(1)		
O(1)a–O(10)c	3.406(2)	O(1)a–*M*(1)–O(10)c	106.5(1)		
O(3)–O(5)b	2.636(2)	O(3)–*M*(1)–O(5)b	84.8(1)		
O(3)–O(6)	2.980(2)	O(3)–*M*(1)–O(6)	90.7(1)		
O(3)–O(9)	2.789(2)	O(3)–*M*(1)–O(9)	79.5(1)		
O(3)–O(10)c	3.043(2)	O(3)–*M*(1)–O(10)c	90.6(1)		
O(5)b–O(9)	2.882(2)	O(5)b–*M*(1)–O(9)	82.4(1)		
O(5)b–O(10)c	3.044(2)	O(5)b–*M*(1)–O(10)c	90.2(1)		
O(6)–O(9)	3.501(2)	O(6)–*M*(1)–O(9)	108.9(1)		
O(6)–O(10)c	2.740(2)	O(6)–*M*(1)–O(10)c	79.6(1)		
<O–O>	3.016	<O–*M*(1)–O>	90.2		
M(2) octahedron					
O(3)–O(5)b	2.836(2)	O(3)–*M*(2)–O(5)b	85.8(1)		
O(3)–O(8)d	3.042(2)	O(3)–*M*(2)–O(8)d	97.0(1)		
O(3)–O(11)c	2.771(2)	O(3)–*M*(2)–O(11)c	84.6(1)		
O(3)–O(12)	2.823(2)	O(3)–*M*(2)–O(12)	88.4(1)		
O(4)b–O(5)b	3.000(2)	O(4)b–*M*(2)–O(5)b	92.3(1)		
O(4)b–O(8)d	2.728(2)	O(4)b–*M*(2)–O(8)d	84.6(1)		
O(4)b–O(11)c	2.802(2)	O(4)b–*M*(2)–O(11)c	86.0(1)		
O(4)b–O(12)	3.106(2)	O(4)b–*M*(2)–O(12)	100.5(1)		
O(5)b–O(11)c	2.782(2)	O(5)b–*M*(2)–O(11)c	84.1(1)		
O(5)b–O(12)	2.703(2)	O(5)b–*M*(2)–O(12)	82.8(1)		
M(3) octahedron					
O(1)a–O(7)	2.829(2)	O(1)a–*M*(3)–O(7)	83.4(1)		
O(1)a–O(9)	2.896(2)	O(1)a–*M*(3)–O(9)	81.9(1)		
O(1)a–O(10)a	3.689(2)	O(1)a–*M*(3)–O(10)a	107.7(1)		
O(1)a–O(13)	2.779(2)	O(1)a–*M*(3)–O(13)	82.2(1)		
O(2)e–O(7)	2.725(2)	O(2)e–*M*(3)–O(7)	80.5(1)		
O(2)a–O(9)	3.041(2)	O(2)e–*M*(3)–O(9)	87.8(1)		
O(2)e–O(10)a	3.086(2)	O(2)e–*M*(3)–O(10)a	85.6(1)		
O(2)e–O(13)	3.484(2)	O(2)e–*M*(3)–O(13)	112.5(1)		
O(7)–O(9)	2.897(2)	O(7)–*M*(3)–O(9)	81.6(1)		
O(7)–O(10)a	3.756(2)	O(7)–*M*(3)–O(10)a	110.2(1)		
O(13)–O(9)	3.083(2)	O(13)–*M*(3)–O(9)	88.8(1)		
O(13)–O(10)a	2.982(2)	O(13)–*M*(3)–O(10)a	81.6(1)		
<O–O>	3.104	<O–*M*(3)–O>	90.3		
Na octahedron					
O(2)a–O(7)b	4.067(2)	x2	O(2)a–*Na*–O(7)b	112.7(1)	
O(2)a–O(7)g	2.725(2)	x2	O(2)a–*Na*–O(7)g	67.3(1)	
O(2)a–O(12)c	4.294(2)	x2	O(2)a–*Na*–O(12)c	111.5(1)	
O(2)a–O(12)i	2.923(2)	x2	O(2)a–*Na*–O(12)i	68.5(1)	
O(7)b–O(12)c	3.384(2)	x2	O(7)b–*Na*–O(12)c	90.3(1)	
O(7)b–O(12)i	3.366(2)	x2	O(7)b–*Na*–O(12)i	89.7(1)	
<O–O>	3.460		<O–*Na*–O>	90.0	
H–bonding					
O(13)–*H*(1)	0.98(4)		*H*(1)...O(8)j	1.89(4)	
O(13)–*H*(2)	0.98(4)		*H*(2)...O(8)b	1.99(4)	
O(13)–O(8)j	2.760(2)		O(13)–*H*(1)–O(8)j	146(4)	
O(13)–O(8)b	2.934(2)		O(13)–*H*(2)–O(8)b	161(4)	
H(1)–*H*(2)	1.52(5)		*H*(1)–O(13)–*H*(2)	102(4)	

Symmetry Operators: a: x–½, $\bar{y}$+½, z; b: x, y–½, $\bar{z}$+½; c: $\bar{x}$+½, y, z–½; d: x+½, $\bar{y}$+½, z; e: $\bar{x}$+½, y, z+½; f: $\bar{x}$+½, y–½, $\bar{z}$; g: $\bar{x}$, $\bar{y}$+½, z–½; h: $\bar{x}$+½, y+½, $\bar{z}$+1; i: x–½, $\bar{y}$, $\bar{z}$+½; j: $\bar{x}$, $\bar{y}$+½, $\bar{z}$+1

$Al + Fe^{3+} \approx 1$, and the final calculation was done with the constraint that $Fe^{3+} + Al = 1.00$ atoms per formula unit *apfu* (Table 5).

Description of the Structure

Cation coordination and site populations

There are three unique *P* sites, each of which is surrounded by four O atoms in a tetrahedral arrangement. The <*P*–O> distances, individual *P*–O distances, O–O distances and O–*P*–O angles (Table 3) fall within the normal ranges observed for the phosphate group (Baur 1974, Griffen & Ribbe 1979). The site-scattering values and mean bond-lengths at the *Na* and *Ca* sites are typical of Na and Ca, respectively, and hence Na and Ca were assigned to these sites. This is in accord with the Na and Ca contents of the formula unit (Table 5), which excludes both the presence of vacancies and Na–Ca disorder over these sites. The refined site-scattering values and <*M*–O> distances for the *M*(1), *M*(2) and *M*(3) sites indicate that these sites are occupied by Mg, Fe^{2+}, Al and Fe^{3+}, as indicated by the analyzed cell-contents (Table 5). The scattering species at these three sites may be combined in the following way to produce two effective scattering species: Mg* = Mg + Al; Fe* = Fe^{2+} + Fe^{3+} + Mn^{2+}. From the refined site-scattering values, site populations for Mg* and Fe* can be assigned. Following this procedure, the individual chemical species were assigned on the basis of mean bond-length after calculating the Fe^{2+} and Fe^{3+} contents of the crystal required for electroneutrality *and* full occupancy of the *M*(1), *M*(2) and *M*(3) sites, as indicated by the site-scattering values. For the *M*(3) site, the refined site-scattering value is only compatible with occupancy by Fe*. Furthermore, the large mean bond-length indicates that all Mn^{2+} in the formula unit (Table 5) occurs at this site, and that the remaining species is Fe^{2+}. For the *M*(1) site, the mean bond-length is compatible only with occupancy by Fe^{2+} and Mg; any Fe^{3+} or Al at this site would lead to a much shorter mean bond-length. Thus the *M*(1) site-populations were assigned as Fe^{2+} and Mg directly from the refined site-scattering value. All remaining cations (Fe^{2+}, Mg, Fe^{3+}, Al) were assigned to the *M*(2) site, in accord with both the refined site-scattering value and the observed mean bond-length. The resultant site-populations are given in Table 6, together with the observed <*M*–O> distances and the analogous sums of the constituent-cation radii. For the *M*(1) site, the agreement is almost exact. For the *M*(2) site, the calculated value is somewhat higher than the observed value. For the *M*(3) site, the calculated value is less than the observed value, but the site populations are assigned such that <*M*(3)–O> has its maximum possible value consonant with the analyzed bulk composition of the

TABLE 4. BOND-VALENCE (*vu*)* TABLE FOR WICKSITE

	P(1)	*P*(2)	*P*(3)	*M*(1)	*M*(2)	*M*(3)	*Ca*	*Na*	*H*(1)	*H*(2)	Σ
O(1)	1.24			0.40		0.37					2.01
O(2)	1.24					0.41	0.21	$0.10^{\times 2}\downarrow$			1.96
O(3)	1.21			0.37	0.40						1.98
O(4)	1.24				0.41		0.26				1.91
O(5)		1.23		0.35	0.36						1.94
O(6)		1.26		0.37			0.34				1.97
O(7)		1.22				0.36	0.21	$0.32^{\times 2}\downarrow$			2.11
O(8)		1.22			0.48				0.20	0.20	2.10
O(9)			1.19	0.23		0.23	0.21				1.86
O(10)			1.19	0.28		0.16	0.15				1.78
O(11)			1.21		0.42		0.31				1.94
O(12)			1.23		0.57		0.09	$0.14^{\times 2}\downarrow$			2.03
O(13)						0.38	0.17		0.80	0.80	2.15
Σ	4.93	4.93	4.82	2.00	2.64	1.91	1.95	1.12	1.00	1.00	

* calculated with the parameters of Brown and Altermatt (1985)

TABLE 5. CHEMICAL COMPOSITION (wt %) AND UNIT FORMULA (*apfu*)* FOR WICKSITE

P_2O_5	42.05	P	6.01
Al_2O_3	0.92		
**Fe_2O_3	6.45	Al	0.18
FeO	24.09	**Fe^{3+}	0.82
MnO	4.19		
MgO	3.77	Fe^{2+}	3.40
CaO	11.20	Mn^{2+}	0.60
Na_2O	2.98	Mg	0.95
^+H_2O	(3.55)		
Total	99.20	Ca	2.03
		Na	0.98
		H_2O	2

* calculated on the basis of 26 anions *pfu*;
** calculated assuming Fe^{3+} + Al = 1.00 *apfu*;
+ calculated assuming 2 H_2O groups *pfu*

TABLE 6. REFINED SITE-SCATTERING VALUES (*epfu*), SITE POPULATIONS (*apfu*) AND OBSERVED AND CALCULATED MEAN-BOND-LENGTHS (Å) IN WICKSITE

	site-scattering	site population	$<M–O>_{calc}$	$<M–O>_{obs}$
M(1)	46.1(2)	1.58 Fe^{2+} + 0.42 Mg	2.134	2.135
M(2)	41.7(2)	0.46 Fe^{2+} + 0.54 Mg + 0.82 Fe^{3+} + 0.18 Al	2.053	2.042
M(3)	52.0(2)	1.40 Fe^{2+} + 0.60 Mn^{2+}	2.172	2.197

crystal (Table 5). Thus the site populations of Table 6 show the best possible agreement with all measured data on the crystal.

The *H* positions were located on difference-Fourier maps and were refined subject to the constraint that the donor–*H* distance is ~0.98 Å. The resulting H-bond geometry (Table 3) is entirely reasonable (Ferraris & Franchini-Angela 1972, Brown 1976, Chiari & Ferraris 1982) for an H_2O group. Furthermore, the acceptor atoms for the H bonds were easily identified. The atom O(8) is the acceptor for *both* H-bonds, and it is apparent from the bond-valence table (Table 4) that this is a reasonable arrangement from a bond-valence viewpoint. Table 4 also shows that both the pattern of order of the cations and the distribution of bond lengths are in accord with the constraint that the bond-valence requirements around all anions and cations in the structure are satisfied.

Structure topology

Wicksite has quite a densely packed structure, and a single view of the structure is not very informative. However, it may be resolved into layers that reveal its structural principles. Figure 1 shows the layer parallel to (001) at $z = 0.25 \pm 0.10$. $M(1)$ and $M(2)$ octahedra share an edge to form $[M_2\phi_{10}]$ dimers. These dimers are canted to both the *a* and *b* axes. The dimers maintain their cant along [010], but reverse it along [100], and are linked into a layer by $P(1)$ and $P(2)$ tetrahedra. Figure 2 shows the layer parallel to (001) at $z = 0 \pm 0.10$. Two $M(3)$ and one *Na* octahedra share edges to form an $[M_3\phi_{14}]$ trimer that is decorated by $P(3)$ tetrahedra linking adjacent free octahedral vertices: $[M_3(PO_4)_2\phi_6]$. The groups cross-link *via* sharing of octahedron–tetrahedron vertices to form a layer of heteropolyhedra. There are two types of hole within this layer: (1) in the first type of hole is the *Ca* site, coordinated by nine adjacent anions; (2) the second type of hole is occupied by the four H atoms that belong to the two adjacent H_2O groups (Fig. 2). This layer can also be described as consisting of two types of parallel chains: (1) a line of $[M_3\phi_{14}]$ trimers, and (2) a chain of edge-sharing $Ca\phi_9$ and PO_4 polyhedra (Fig. 2). The $Ca\phi_9$ polyhedron shares faces with adjacent $M(3)$ and *Na* octahedra, and an edge with an adjacent $M(3)$ octahedron. The layers of Figures 1 and 2 link by edge-sharing between octahedra. The $M(1)$ octahedron of one sheet (Fig. 1) shares an edge with the $M(3)$ octahedron (Fig. 2), as shown in Figure 3.

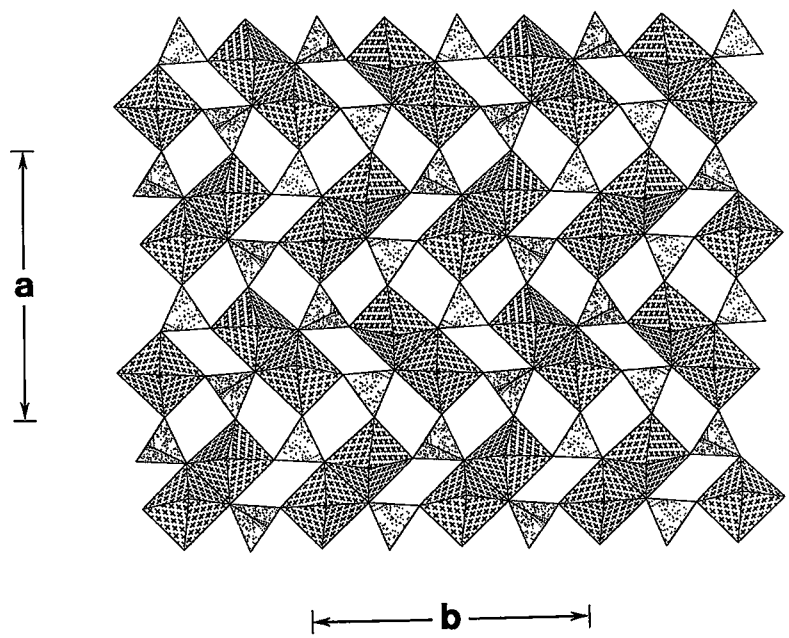

FIG. 1. The structure of wicksite: the layer parallel to (001) at $z = 0.25 \pm 0.10$; phosphate tetrahedra are shaded with a random-dot pattern, $M(1)$ and $M(2)$ octahedra are shaded with crosses.

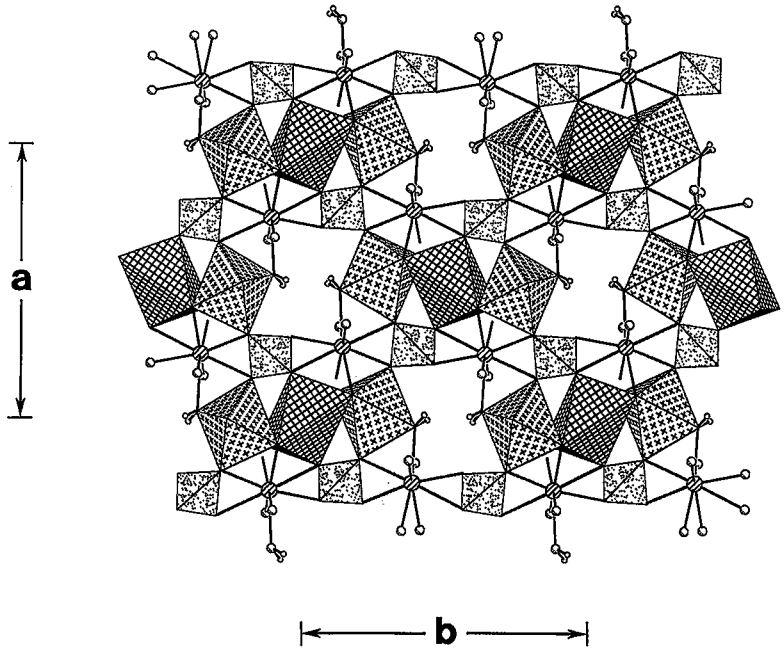

FIG. 2. The structure of wicksite: the layer parallel to (001) at $z = 0 \pm 0.10$; $M(3)$ octahedra are shaded with crosses, *Na* octahedra are shaded with a 4^4-net, miscellaneous O-atoms are shown as small highlighted circles, H atoms are shown as small circles, Ca atoms are shown as large circles with diagonal-line shading.

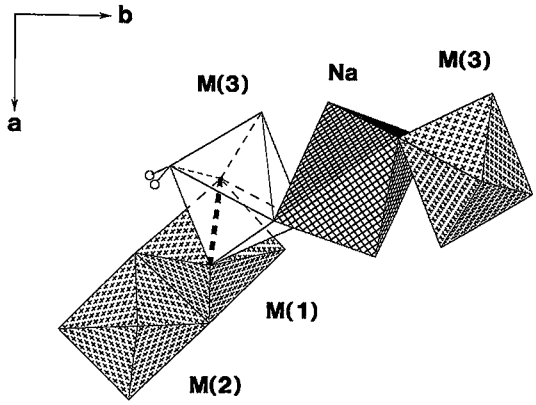

FIG. 3. The $M(1)$=$M(2)$ dimer of Figure 1 and the $M(3)$=*Na*=$M(3)$ trimer of Figure 2 linking *via* edge-sharing between the $M(1)$ and $M(3)$ octahedra in wicksite; legend as in Figures 1 and 2, except that one of the $M(3)$ octahedra is unshaded in order to see the shared edge that is marked by a heavy broken line; the positions of the H atoms are shown by small circles.

Figure 4 shows the layer parallel to (100) at $x = 0 \pm 0.12$. The $[M_3\phi_{14}]$ trimer of Figure 2 is also very prominent here, and shows the same rows of trimers in this projection; however, note that the flanking $P(3)$ tetrahedra (*cf.* Fig. 2) are not shown in this layer. Between the discontinuous rows of trimers are rows of phosphate tetrahedra that are modulated according to the cants of the adjacent trimers of octahedra. The trimer is terminated at each end by an H_2O group. The H atoms lie approximately in the plane of this layer, and form H-bonds with the O(8) atoms of two adjacent $P(2)O_4$ tetrahedra (shown by heavy broken lines in Fig. 4). Figure 5 shows the layer parallel to (100) at $x = 0.25 \pm 0.15$. The $M(1) = M(2)$ dimers of Figure 1 are also prominent in this view. Adjacent vertices are bridged by tetrahedra forming $[M_2(TO_4)\phi_6]$ chains along [001] at $y \approx 0.15$ and 0.65. These chains cross-link in the *b*-direction *via* corner-sharing between the dimer octahedra and additional phosphate tetrahedra, with Ca occupying the interstices within this layer (Fig. 5).

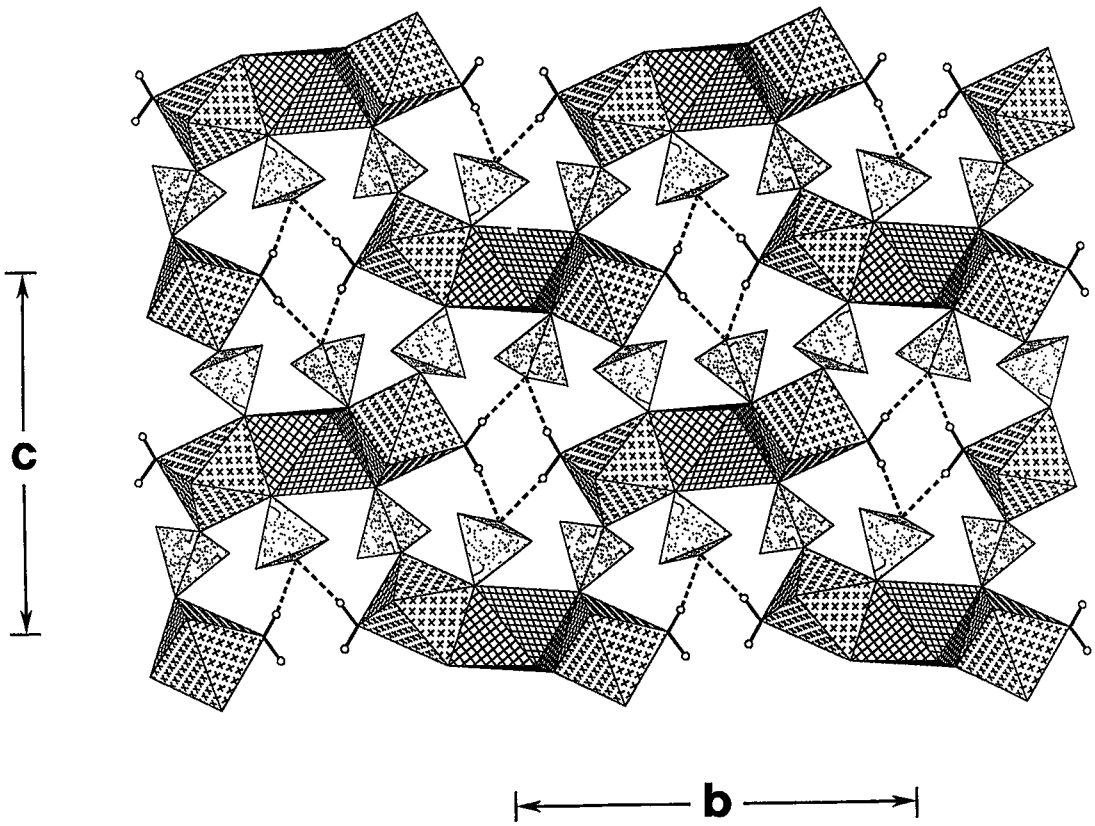

FIG. 4. The structure of wicksite: the layer parallel to (100) at $x = 0 \pm 0.12$; legend as in Figures 1 and 2, H bonds are denoted by heavy broken lines.

Related minerals

Wicksite, ideally $NaCa_2Fe^{2+}{}_4(MgFe^{3+})(PO_4)_6(H_2O)_2$, is isostructural with grischunite, ideally $NaCa_2Mn^{2+}{}_4(Mn^{2+}Fe^{3+})(AsO_4)_6(H_2O)_2$. Grischunite was described by Graeser *et al.* (1984), and the structure was solved by Bianchi *et al.* (1987). The isostructural nature of these two minerals escaped notice. Other wicksite-like phases were reported by Peacor *et al.* (1985) and Ek & Nysten (1990). The phase of Peacor *et al.* (1985) has 2.22 Fe^{3+} *pfu*, 0.27 Na *pfu* and 4.80 (H_2O) *pfu* on the basis of approximately 6 (PO_4) groups *pfu*. Analogous values for wicksite are 1.00 (Fe^{3+} + Al) *pfu*, 0.98 Na *pfu* and 2.00 (H_2O) *pfu*. The values given by Peacor *et al.* (1985) are very unlike those of wicksite, and also incompatible with the wicksite structure. Hence this phase is not isostructural with wicksite. Ek & Nysten (1990) reported another wicksite-like phase similar to that described by Peacor *et al.* (1985). Again, this material has 4 (H_2O) *pfu* instead of the 2 (H_2O) required by the wicksite structure, and must be a distinct phase.

As noted above, we suspected that wicksite and grischunite might be monoclinic, this lower symmetry being induced by ordering of Mg and Fe^{3+} (Mn^{2+} and Fe^{3+} for grischunite) over nonequivalent sites in a monoclinic structure. Both structures were successfully refined in monoclinic symmetry, but the results did not show significant differences from the orthorhombic models. However, Sturman *et al.* (1981) did note that "many grains of wicksite show anomalous optical effects consistent with monoclinic, rather than orthorhombic symmetry." Thus, like its namesake, wicksite is suspected of deviant behavior but it cannot be proven.

ACKNOWLEDGEMENTS

We thank Professor Dr. Stefan Graeser for supplying us with crystals of grischunite, and Drs. Peter Burns and Don Peacor for their reviews of this paper. We are grateful to The Emerald Goddess for supplying us with wicksite, sample number M37364, from the collection of the Royal Ontario Museum. Financial support was provided by the Natural Sciences and Engineering Research Council of Canada.

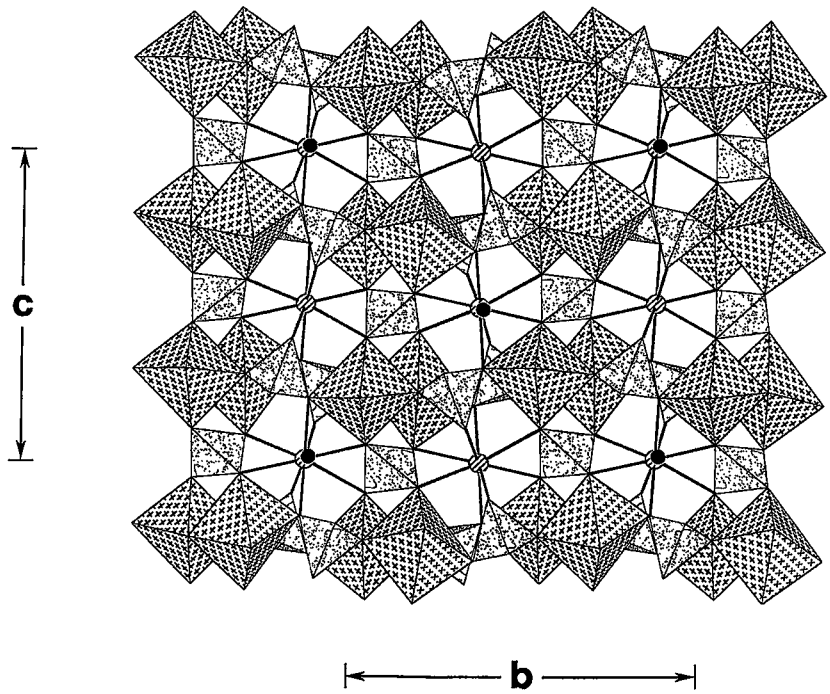

FIG. 5. The structure of wicksite: the layer parallel to (100) at $x = 0.25 \pm 0.15$; legend as in previous figures, the H_2O group is shown as a black circle.

REFERENCES

BAUR, W.H. (1974): The geometry of polyhedral distortions. Predictive relationships for the phosphate group. *Acta Crystallogr.* **B30**, 1195-1215.

BIANCHI, R., PILATI, T. & MANNUCCI, G. (1987): Crystal structure of grischunite. *Am. Mineral.* **72**, 1225-1229.

BROWN, I.D. (1976): On the geometry of O–H...O hydrogen bonds. *Acta Crystallogr.* **A32**, 24-31.

_____ & ALTERMATT, D. (1985): Bond-valence parameters obtained from a systematic analysis of the inorganic crystal structure database. *Acta Crystallogr.* **B41**, 244-247.

CHIARI, G. & FERRARIS, G. (1982): The water molecule in crystalline hydrates studied by neutron diffraction. *Acta Crystallogr.* **B38**, 2331-2341.

EK, R. & NYSTEN, P. (1990): Phosphate mineralogy of the Hålsjöberg and Hökensås kyanite deposits. *Geol. Fören. Stockholm Förh.* **112**, 9-18.

FERRARIS, G. & FRANCHINI-ANGELA, M. (1972): Survey of the geometry and environment of water molecules in crystalline hydrates studied by neutron diffraction. *Acta Crystallogr.* **B28**, 3572-3583.

GRAESER, S., SCHWANDER, H. & SUHNER, B. (1984): Grischunit $CaMn_2(AsO_4)_2$, eine neue Mineralart aus den Schweizer Alpen. *Schweiz. Mineral. Petrogr. Mitt.* **64**, 1-10.

GRIFFEN, D.T. & RIBBE, P.H. (1979): Distortions in the oxyanions of crystalline substances. *Neues Jahrb. Mineral., Abh.* **137**, 54-73.

HAWTHORNE, F.C., UNGARETTI, L., OBERTI, R., BOTTAZZI, P. & CZAMANSKE, G. (1993): Li: an important component in igneous alkali amphiboles. *Am. Mineral.* **78**, 733-745.

PEACOR, D.R., DUNN, P.J., RAMIK, R.A., CAMPBELL, T.J. & ROBERTS, W.L. (1985): A wicksite-like mineral from the Bull Moose mine, South Dakota. *Can. Mineral.* **23**, 247-249.

ROBERTSON, B.T. (1982): Occurrence of epigenetic phosphate minerals in a phosphatic iron formation, Yukon Territory. *Can. Mineral.* **20**, 177-187.

ROBINSON, G.W., VAN VELTHUIZEN, J., ANSELL, H.G. & STURMAN, B.D. (1992): Mineralogy of the Rapid Creek and Big Fish River area, Yukon Territory. *Mineral. Rec.* **23**, 1-47.

STURMAN, B.D., PEACOR, D.R. & DUNN, P.J. (1981): Wicksite, a new mineral from northeastern Yukon Territory. *Can. Mineral.* **19**, 377-380.

YOUNG, F.G. (1977): The mid-Cretaceous flysch and phosphatic ironstone sequence, northern Richardson Mountains, Yukon Territory. *Geol. Surv. Can., Pap.* **77–1C**, 67-74.

Received January 10, 1997, revised manuscript accepted March 12, 1997.